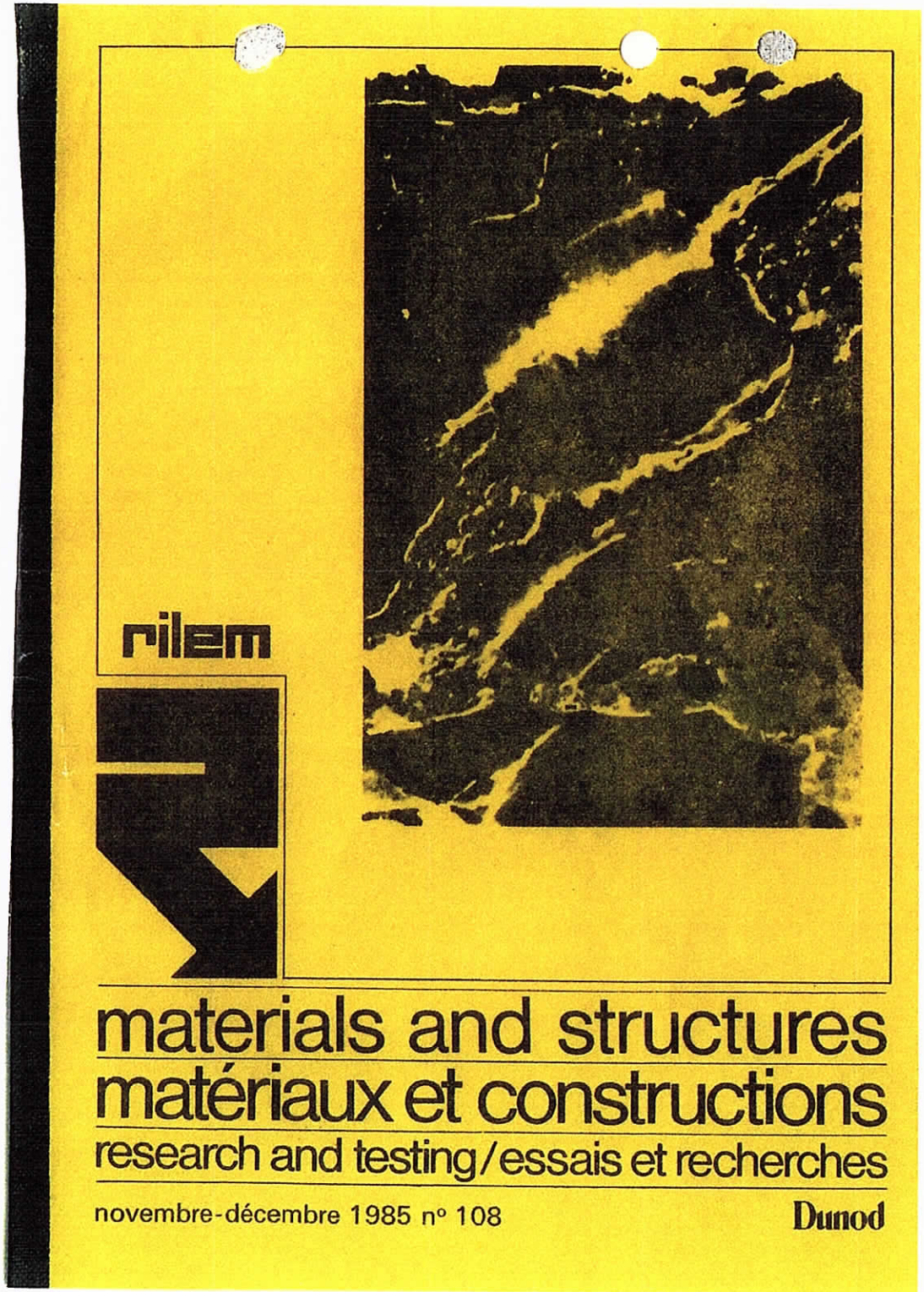

Fracture analysis of the pullout test

H. Krenchel

Associate Professor, Department of Structural Engineering, Denmark Technical University, Lyngby, Denmark.

S. P. Shah

Professor of Civil Engineering, Northwestern University, Evanston, Il., USA.

Pullout tests are increasingly being used to determine the in situ *strength of concrete. Several studies have shown that a close correlation exists between the maximum pullout load and compressive strength of concrete. However, the failure mechanism of the pullout test is yet not understood. Conflicting theories have been forwarded to analyze the pullout test.*

In this study, progressive internal microcracking was examined during the pullout testing. A commercially available equipment was modified to enable monitoring the pullout load vs. relative displacement relationship. Specimens were loaded and unloaded from predetermined fractions of the ultimate load. Acoustic activity was measured during testing. Unloaded specimens were sectioned and examined for microcracking.

Results indicate a two-stage cracking process. An extensive stable cracking system dominates for loads up to than the peak load. A different cracking pattern develops near the peak load and governs the shape of the finally extracted core.

INTRODUCTION

Pullout testing of concrete to determine its in-place strength was first suggested by a Russian scientist nearly 50 years ago [1]. This idea was later extensively explored by Kierkegaard-Hansen of the Technical University of Denmark ([2], [3]). The pullout test system that he suggested is shown in figure 1 and is often referred to as the LOK-TEST. A 25 mm diameter, stiff steel disc is cast into concrete 25 mm below the concrete surface. At a desired interval after casting, this disc is loaded along its axis in the direction of the test surface by means of a pullout jack placed on the surface with circular seating (*fig.* 1). The diameter of the pullout disc, the depth of embedment and the diameter of the support ring were selected so as to obtain a linear relation between the pullout load and the corresponding independently measured uniaxial compressive strength. Many investigators have used this LOK-TEST system and have reported an essentially linear relationship between the compressive strength and the pullout load for a wide range of parameters that can influence compressive strength (type of cement, curing conditions, age at testing, type of aggregates, and mix proportions for example) ([4], [5]). Similar relationships between compressive strength and the pullout load have also been reported by other comparable pullout test systems ([6], [7]).

This empirically observed close correlation between the pullout load and the concrete compressive strength have led to many investigations concerning the actual mode of failure inside the concrete during the pullout loading ([8] to [12]). In 1976, Jensen and Braestrup [8] using the rigid ideal plasticity theory derived a direct relationship between pullout force and compressive strength. The extracted section of concrete was assumed to be a truncated cone with the failure plane running from the outer periphery of the disc towards the inner

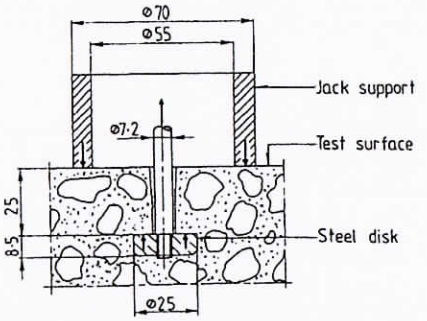

Fig. 1. — Pullout test arrangement in the so-called LOK-TEST system. (All dimensions: mm.)

0025-5432/85/06 439 07/$ 2.70/

periphery of the support ring. They used a modified Coulomb failure criterion. Ottosen has carried out a nonlinear finite element analysis of the pullout test. His constitutive model for concrete is based on nonlinear elasticity and on failure criterion which was dependent on all three invariants of the principal stresses. His analysis indicated that the failure surface of the concrete cone is completely formed at approximately 65% of the ultimate load. The reserve pullout capacity beyond 65% was attributed to the formation and crushing of a compressive strut along a narrow band between the disc and the support.

To better understand the failure mechanism during a pullout test, Stone and Carino conducted two large-scale pullout tests. To facilitate measurements of strains in concrete, they enlarged the scale by approximately 12: 1. The internal strains in three mutually perpendicular directions were measured along the surface obtained by joining the disc and the reaction ring by specially designed micro-embedment strain gages. They concluded that circumferential cracking is completed at about 60 to 70% of the failure load. Observed compressive strains adjacent to the conical failure surface were insufficient to initiate compressive failure. Large tensile strains perpendicular to the failure surface existed near the outer edge of the disc. They attributed the additional capacity beyond 60 to 70% of maximum load to the aggregate interlock.

It should be noted that although the dimensions of the test specimens were enlarged about 12 times in the tests reported by Stone and Carino, the maximum size of aggregate was not scaled up (1/4 inch maximum size was used). It is possible that their observations may not entirely correspond to the conventional pullout test because the fracture processes in concrete are sensitive to the relative dimensions of specimens and the maximum size of the aggregates ([13], [14]). For the study reported in this paper, fracture processes were studied using conventional pullout tests (*fig.* 1).

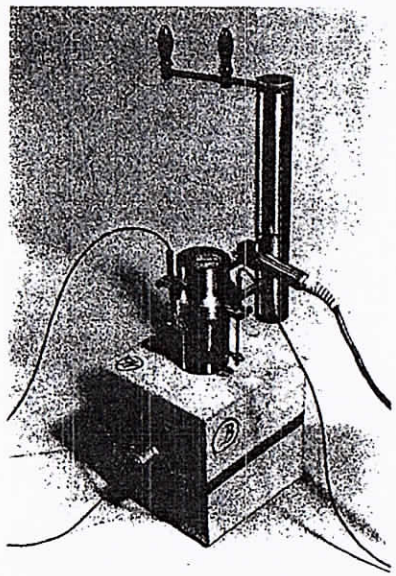

Fig. 2. — Pull-out jack equipped with oil pressure load cell and two displacement transducers.

TESTING APPARATUS

Specimens were loaded using a standard LOK-TEST equipment up to a predetermined fraction of the maximum load, unloaded, sectioned and microscopically examined. Measurements of load, displacement and the acoustic emission (AE) were made during loading.

To enable measurements of load and displacement during both the ascending and the descending parts of the load-displacement curves, the pull-out jack was equipped with an oil pressure transducer in the hydraulic system and with two displacement transducers to measure the relative displacement between the jack (the counterpressure ring or support) and the top end of the pullout bolt and its coupling unit, as shown in figure 2.

The oil pressure was measured with a Hottinger Baldwin (HBM) pressure transducer, type P3M/500 (500 bar full scale), connected to an HBM type KWS 3050 strain indicator. The displacement was recorded by a pair of RDP inductive transducers, type D5/40g8 (± 1 mm) and the DRF type "Dataspan 2000" measuring system.

The acoustic emission (AE) was detected with a system consisting of a transducer, a preamplifier and a monitoring unit. The transducer tuned to about 100 kHz, and consisted of a piezoelectric crystal disc, 16 mm diameter by 5 mm height, with a 6 mm steel disc at top and bottom, all cast into an acrylic cylinder (26 mm diameter by 32 mm). The preamplifier was a Dunegan/Endevco, type 801P. The monitoring unit was type ABK-AEI, set to measure the acoustic activity (AA, counts per second).

These three parameters (load, displacement and AA) were recorded on an x-y_1-y_2 recorder, HP type 7046A, with the displacement along the x-axis and the load (oil pressure) and acoustic activity along the y_1-and y_2-axis, respectively.

The pullout discs were cast in 20 cm concrete cubes. The pullout loading was affected centrally in one of the side faces of the cube (side face during casting of the concrete), and the AE-transducer was placed centrally on one of the other side faces (*fig.* 2).

Concrete test specimens

A total of ten 20 cm cubes, plus five control cylinders, 15 cm diameter by 30 cm, were cast for the test program, all from the same batch of concrete. A standard pullout disc (25 mm diameter by 8.5 mm) was mounted on its stem in the normal way, at the center of two opposite side faces in each cube.

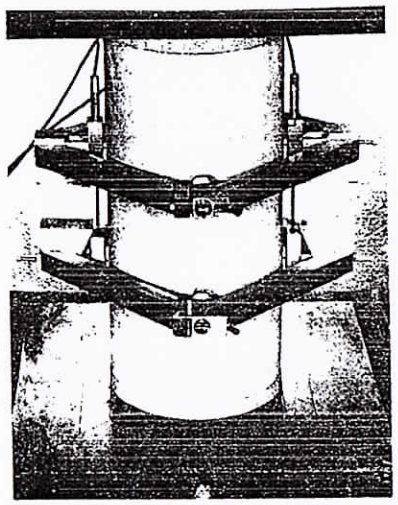

Fig. 3. — Concrete cylinder 150 mm diameter by 30 cm with longitudinal strain measuring equipment (l_0 = 100 mm).

The concrete used had a w/c-ratio of 0.74, with maximum aggregate grain size 18 mm and volume ratio of paste to aggregate: 23/77. The concrete mix proportions are given in table I. All the concrete was vibrated into the moulds (Vebe-time 8 sec.). The concrete was vibrated by fixing one mould at a time to a vibration table and slowly pouring in the concrete.

A two stage curing was used for all test pieces: the test places were kept moist for 1 week (95% RH and 20°C) followed by 2 weeks in laboratory atmosphere (50% RH and 20°C) untill the day of testing.

Testing program

On the day of testing the cylinders were loaded in uniaxial compression, two of them for compression strength testing, and three with longitudinal strain measuring equipment over the mid-span of 100 mm for stress/strain registration, see figures 3 and 4. The material properties of the concrete are given in table II. The 20 pullout tests were carried out as follows:

Six of the tests were conducted with a monotonically increasing pullout load. Tests were conducted until the load corresponding to about 25% of the peak load in the descending part was reached (*fig.* 5). For two of these tests only the load/displacement curve was recorded, whereas for the four of them, acoustic activity was also monitored (*fig.* 5).

The remaining 14 pullout tests were carried out with only partial loading, followed by unloading. This made it possible, when the concrete blocks were later cut

TABLE I

CONCRETE MIX PROPORTIONS 1 m³ batch recipe

	kg	l
Cement (rapid hardening)	205	61
Gravel (sea bed: 0-8 mm)	908	347
Granit (broken: 8-18 mm)	1 156	420
Water	152	152
Air (approx.)	0	20
TOTAL	2421	1000

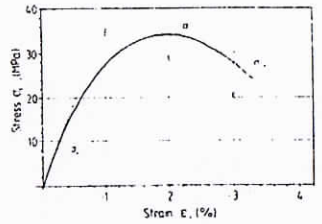

Fig. 4. —Stress/strain curve in uniaxial compression. Concrete cylinder No. 5.

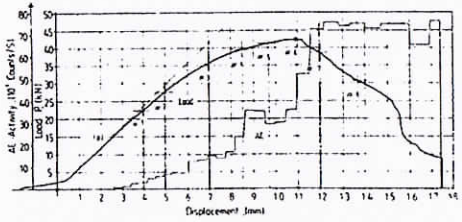

Fig. 5. — Complete load/displacement curve with AE-registration. (Concrete cube No. 17.) Load level shown of test No. 1-8, taken out for micro crack examination.

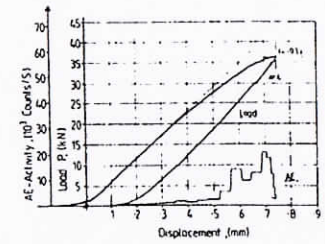

Fig. 6. — Load/displacement curve test No. 4, de-loaded from load level: 93% of average peak load.

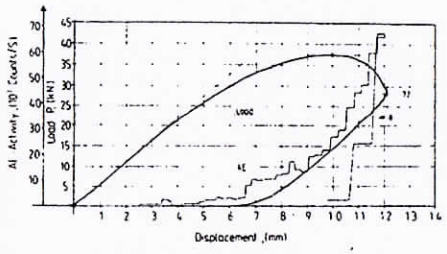

Fig. 7. — Load-displacement curve test No. 8, de-loaded from load level at descending branch: 72% of peak load.

through the axial plane of the pullout bolts, to examine the step-by-step development of the internal microcracking in the concrete in the stressed zone between the pullout disc and the support-surface of the concrete.

In five of these tests the specimens were unloaded after reaching different levels of loads before the peak (*fig.* 6), while another five were unloaded from different levels during the descending part of the load/displacement curve (*fig.* 7). Two of the tests were loaded just to the peak and were then unloaded.

As soon as each test had been completed and the pullout jack removed, the concrete surface where the jack had been placed was thoroughly examined for any visible cracking.

The test surfaces from the five tests mentioned first and from the two mentioned last, taken just to the peak load, showed no cracking at all, but only a slightly shiny, circular ring mark (55 mm diameter and 70 mm diameter), where the pullout jack had stood. By placing a sharp steel ruler on the surface of the concrete along a diameter and shining light in from behind it could be seen that no measurable pulling out had taken place in any of these seven loading tests.

In the remaining five tests, on the other hand, in which unloading had been carried out from different levels after the peak had been reached, the test surface showed a clear circumferential crack along the inside of the support (55 mm diameter), and here it was obvious that noticeable pulling out had taken place. By placing the above-mentioned steel ruler on the concrete surface, it was possible to measure the pullout displacement relative to the rest of the concrete surface. The displacement was about 0.1 mm when unloading had taken place just after the peak had been passed, and about 1 to 2 mm when the test had been carried through to the utmost, but in none of the cases had the pullout cone come out by itself.

A total of eight test pieces were then selected for examination of the internal cracking and its development at the different loading levels: five from the ascending part of the loading curve (loading levels 53, 65, 84, 93 and 97% of ultimate load), one from the peak (100%), and two from the descending part of the curve (91 and 72% of the ultimate load).

Study of internal cracking

The concrete blocks selected for examination were cut with a diamond saw (700 mm diameter by 5 mm), with two incisions at each pullout disc. The first cut was made parallel to the concrete test (support) surface 0.5 mm below the pullout disc. The second cut was placed so that one of the two cutting planes passed exactly through the pullout axis, and this diametrical plane on the cut-out blocks was then used for the following crack examination.

Just after cutting and while still wet, the concrete blocks (34 by 100 mm) were placed in alcohol for 16 hours and were then dried out gently and vacuum-treated for epoxy impregnation.

The epoxy resin used was a cold-setting, low viscosity type (Ulfear type A 180 with hardener H 85), containing 1.1% by weight of fluorescent dye (Hudson Yellow Dye). When fully hardened, the surface was ground and polished (in seven steps, down to No. 1200 silicon carbide) [15].

The polished surface was illuminated by a halogen lamp through a blue-red filter and was observed through a red-yellow filter, which gave maximum contrast between the cement paste (light red), the aggregate particles (dark red), and cracks (yellow).

The cracks were examined first with the naked eye and then in direct photography. The latter technique

TABLE II

CONCRETE MATERIAL PROPERTIES (see *fig.* 4)

Cylinder nr.	1	2	3	4	5	Average
Density (kg/l)	2.4409	2.4277	2.4541	2.4560	2.4616	2.4481
f_c' (MPa)	31.48	33.06	32.89	35.17	33.82	33.28
E_0 (GPa)	—	—	35.1	37.60	37.7	36.8
σ_p (MPa)	—	—	10.0	10.1	8.1	9.4
ε_u (%)	—	—	0.212	0.160	0.210	0.194
$\sigma_{\varepsilon_t\,0.3\%}$ (*) (MPa)	—	—	31.8	—	27.8	29.8

(*) Load on descending part of the stress/strain-curve at a total strain : $\varepsilon_{tot} = 0.30\%$ (see *fig.* 4).

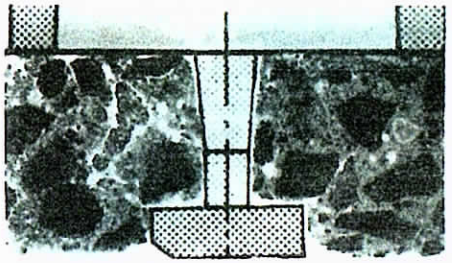

Fig. 8. — Crack analysis No. 1, load level: 53% of average load.

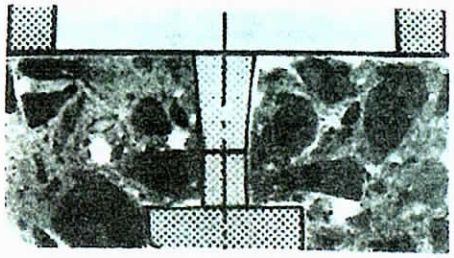

Fig. 12. — Crack analysis No. 5, load level: 97% of average peak load.

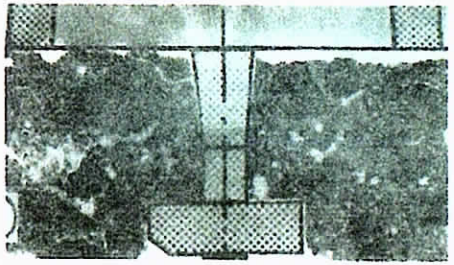

Fig. 9. — Crack analysis No. 2, load level: 65% of average peak load.

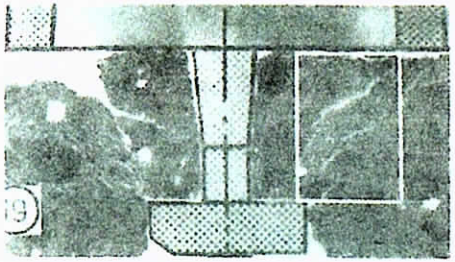

Fig. 13. — Crack analysis No. 6, de-loaded from peak of load displacement curve. (Area for closer examination shown, cf. fig. 18.)

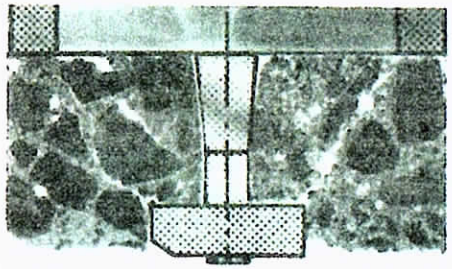

Fig. 10. — Crack analysis No. 3, load level: 84% of average peak load.

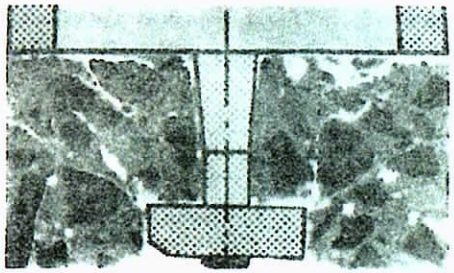

Fig. 14. — Crack analysis No. 7, de-loaded from the descending branch at load level: 91% of peak load.

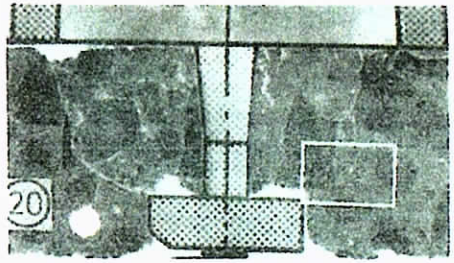

Fig. 11. — Crack analysis No. 4, load level: 93% of average peak load. (Area for closer examination shown, cf. fig. 17.)

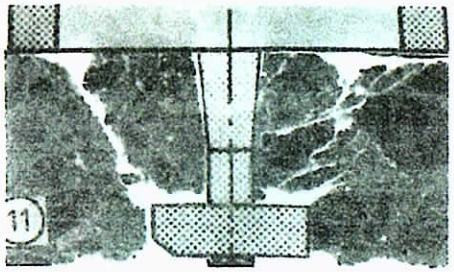

Fig. 15. — Crack analysis No. 8, de-loaded from the descending branch at load level: 72% of peak load.

Fig. 16. — Close microscope examination of selected area, crack analysis No. 4 (see fig. 12). In scale 1:1 this area was 9.7 × 14.5 mm.

gives sharp reproduction for a total enlargement of up to about 10 times, with clear detection of cracks with widths down to 0.01 to 0.05 mm (*fig.* 8 through 15).

In selected areas, a stero-microscope with a magnification of 20 was used. With this, any crack down to crack widths of 1 to 5 μm can be observed (*fig.* 16 and 17).

RESULT

From the comparison with the measurement of the acoustic emission activity, the following observations can be made regarding the internal fracture mechanism in these pullout tests:

1. Acoustic emission starts at the limit of proportionality of the load/displacement curve. The development of the AE-activity versus load all the way up to the peak is a typical exponential function (see *fig.* 18), similar to the deviation of uniaxal compressive the load/displacement curve from its initial tangent (*fig.* 4).

2. Microcracking detected by AE-activity, starts at a rather early loading level, about 30% of the peak load (23 to 36%).

3. After the peak there is a drastic rise in AE-activity, with a factor of about 2 (1.4 to 2.3) in comparison with the activity level at the peak.

4. When unloading takes place from the peak, or immediately after this, no noticeable pulling out has occurred. The tested concrete surface is uncracked and still plane.

5. Numerous microcracks occur in the concrete during loading, parallel to the development of AE-activity. The cracks normally start in the mortar and at the mortar/aggregate interface. At higher loading levels, some of the cracks also pass through the aggregate particles (see *fig.* 8 through 13).

6. At the lower levels (up to about 65% of the peak load) cracking seems to be primarily concentrated near the pullout disc. At higher levels (near the peak load)

Fig. 17. — Close microscope examination of selected area, crack analysis no. 6 (see fig. 14). In scale 1:1 this area was 16.2 × 24.3 mm.

cracks are also observed near the underside of the counter-pressure support.

7. The main direction of the cracks that are observed for loads up to the peak is such that the apex angle (the angle between the pullout axis and the direction of the crack) is 70 to 80°. This system of cracking is termed primary.

8. A secondary cracking system form with a smaller apex angle (approximately 30°) starting from the upper edge of the disc and going toward the inside edge of

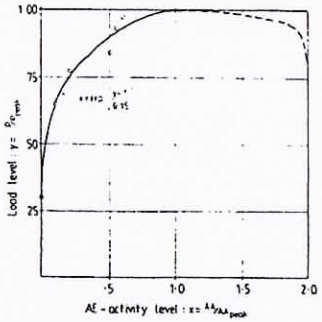

Fig. 18. — Acoustic emission activity level versus load level with exponential regression curve to the peak.

the support. This secondary cracking system did not develop fully until after the peak of the load-displacement curve had been passed.

9. Most of the cracks in the principal cracking system are extremely fine, being only visible under a microscope. Even at the highest loading levels the crack width here is in most cases only about 0.01 mm or less. The secondary cracking system, on the other hand, which is observed primarily beyond the peak, is visible to the naked eye with a crack width of approximately 0.2 mm.

10. At the peak (see *fig.* 13), the predominant cracking pattern is still the primary (principal) pattern described above (point 7). After that, the secondary crack described in point 8 forms all the way around, simultaneously with the discontinuous rise in AE-activity described in point 3.

DISCUSSION

The fracture process during the pullout test seems to consist of two systems of cracking: principal cracking system and secondary cracking system. The principal cracks initiate at about 30% of the peak load, near the upper corner of the disc. The apex angle of this system of cracking is much larger than the reported angle of the final extracted cone. The principal cracking system dominates for loads less than the peak load and appears to be a stable system.

It is interesting to note that the cracking pattern similar to the principal cracks observed here has been also reported experimentally for plane-stress pullout tests conducted at Northwestern University by Ballarini, Shah and Keer [16]. By using linear elastic fracture mechanics they were able to predict the observed direction of cracking. These cracks originate at the upper corners of the disc due to high Mode I stress intensity factor, but become stable before the peak load is reached. This was true for the test geometry corresponding to the LOK-TEST. However, as the support reactions were moved further apart, the principal cracks became unstable.

The apex angle observed here for the secondary crack roughly corresponds to the angle of the finally extracted cone. The development of the secondary cracking system seems to coincide with the observed sharp increase in acoustic activity.

The mechanism of transition from the stable principle cracking system to the secondary cracking system is probably complex involving considerations such as nonlinear fracture mechanics, mixed mode crack propagation, increasing compressive stress field as the cracks approach the support ring and the aggregate interlock effects. However, from this study it is apparent that the failure mechanism based solely on the shape of the extracted cone is not appropriate in predicting the peak load. For predicting the ultimate load, the formation and direction of the principle cracking system must be considered.

ACKNOWLEDGMENT

The authors appreciate support from NATO Science Division (Research Grant No. 702/84).

REFERENCES

[1] Skramtajev B. G. — *Determining concrete strength for control of concrete structures.* Proceedings, American Concrete Institute, Vol. 34, 1938.

[2] Kierkegaard-Hansen P. — *LOK-strength.* Nordisk Betong, Stockholm, Sweden, No. 3, 1975, pp. 19-28.

[3] Kierkegaard-Hansen P., Bickley J. A. — *In situ strength evaluation of concrete by the LOK-test system,* presented at the American Concrete Institute Fall Convention, Houston, Tex., USA, Oct. 29-Nov. 3, 1978.

[4] Krenchel H., Bickley J. A. — *Concrete pullout test methods. Historical background and scientific level today,* presented at the American Concrete Institute Annual Convention, Phoenix, Ariz., USA, March 4-9, 1984.

[5] Krenchel H., Petersen C. G. — *In situ testing with LOK-test, ten years experience.* Proceedings of the International Conference on In situ/Non Destructive testing of Concrete, CAMMET, Ottawa, Ontario Canada, Oct. 2-5, 1984.

[6] Malhotra V. M. — *Evaluation of the pullout test to determine strength of in situ concrete.* Materials and Structures (RILEM, Paris), Vol. 8, No. 43, Jan-Feb. 1975, pp. 19-31.

[7] Richars O. — *Pullout strength of concrete, reproducibility and accuracy of mechanical tests.* STP-626, ASTM, Phila., 1977, pp. 32-40.

[8] Jensen B. C., Braestrup M. W. - *LOK-tests determine the compressive strength of concrete.* Nordisk Betong, Stockholm, Sweden, No. 2, 1976, pp. 9-11.

[9] Ottosen N. S. - *Nonlinear finite element analysis of pullout test.* Journal of the Structural Division, Proceedings of the American Society of Civil Engineers, Vol. 107, No. ST4, April 1981, pp. 591-603.

[10] Stone W. C., Carino N. J. *Deformation and failure in large-scale pullout tests.* Technical Paper No. 80-46, ACI Journal, Nov-Dec. 1983, pp. 501-513.

[11] Yener M., Chen W. F. - *On in-place strength of concrete and pullout tests.* Cement Concrete and Aggregates, Vol. 6, No. 2, Winter 1984, pp. 96-99.

[12] Stone W. C., Giia J. — *The effect of geometry and aggregate on the reliability of the pullout test.* Concrete International, Vol. 7, No. 2, Feb. 1985, pp. 27-36.

[13] Jeng Y. S., Shah S. P. - *A fracture toughness criterion for concrete.* International Journal of Engineering Fracture Mechanics, Vol. 20, No. 3, pp. 1055-1069.

[14] Wecharatana M., Shah S. P. — *Prediction of nonlinear fracture process zone in concrete.* Journal of Engineering Mechanics, ASCE, Vol. 109, No. 5, Oct. 1983, pp. 2231-1246.

[15] Monsted K., Thorsen T. - *Interference fluorescence analyses of cracks.* DIA-LOG, 20th anniversary 77, Danmarks Ingeniorakademi, Bygningsafdelingen, Lyngby, Denmark, 1977, pp. 213-222.

[16] Ballarini R., Shah S.P. and Keer L.M. — *Pullout failure of anchor bolts,* paper No 85A65, Proceedings of the Royal Society of London (in press).

RÉSUMÉ

Étude de rupture de l'essai d'arrachement. — *On se sert de plus en plus des essais d'arrachement pour déterminer la résistance du béton en œuvre. Plusieurs études ont montré une corrélation étroite entre l'effort d'arrachement maximal et la résistance en compression du béton. Pourtant, le mécanisme de rupture de l'essai d'arrachement n'est pas encore bien compris, et des théories divergentes ont été avancées à titre d'explication.*

Au cours de cette étude, on a procédé à l'examen de la propagation des microfissures internes durant l'essai. Un appareil disponible sur le marché a été modifié afin de permettre le contrôle de l'effort d'arrachement. Compte tenu de sa relation avec le déplacement relatif, les corps d'épreuves ont été chargés et déchargés par fractions prédéterminées de la charge de rupture, on a procédé à une auscultation acoustique au cours de l'essai. Les corps d'épreuve déchargés ont été sectionnés et soumis à un examen de micro-fissuration.

Les résultats indiquent un processus de fissuration en deux étapes. On constate la prédominance d'un système de fissures stables et étendues pour les efforts exercés jusqu'à la valeur de pointe et au-dessus. Une configuration différente de fissures apparaît près de la valeur de pointe et détermine la forme du noyau finalement extrait.